

Ionization and Velocity Structure in the Supernova Remnant E0102-72

K.A. Flanagan, C.R. Canizares, D.S. Davis, D. Dewey, J.C. Houck, T.H. Markert, M.L. Schattenburg

*Center for Space Research, Massachusetts Institute of Technology,
77 Massachusetts Ave., Cambridge, MA 02139*

Abstract. The High Energy Transmission Grating (HETG) Spectrometer aboard the Chandra X-Ray Observatory was used to observe E0102-72, a ~ 1000 year old, oxygen rich supernova in the Small Magellanic Cloud. The HETG disperses the image of the remnant into a spectrum of images in the light of individual X-ray emission lines. Doppler shifts in the strongest lines of oxygen and neon reveal bulk motions of up to 2000 km/sec with a complex morphology. Comparison of progressive ionization stages of magnesium, neon, oxygen and silicon provide new insights into the mechanism of the ‘reverse shock’ that heats the stellar ejecta.

1. Introduction

1E0102.2-7219 is a young (~ 1000 years) supernova remnant (SNR) in the Small Magellanic Cloud. It was discovered in X-rays with the *Einstein* Observatory (Seward & Mitchell 1981), and shortly afterwards optical filaments of oxygen were found (Dopita et al. 1981) and measured to have velocities of thousands of km/s (Tuohy & Dopita 1983), pegging it as one of a small number of identified oxygen-rich SNRs. As a class, these SNRs are believed to come from supernovae with massive progenitors, exhibit high velocities in their optical filaments, are young (with the possible exception of Puppis A) and often show evidence of asymmetrical explosion. E0102-72 has been observed in UV (Blair et al. 1989; Blair et al. 2000) and radio (Amy & Ball 1993), and in the X-ray with *Chandra* and other X-ray observatories (Hayashi et al. 1994; Gaetz et al. 2000; Hughes et al. 2000). Based on early X-ray observations, Hughes (1988) ruled out a uniform-density shell model. Our data (Houck et al. 2000) and Gaetz et al. (2000) confirm Hughes’ conclusion. Gaetz et al. (2000) have looked at direct *Chandra* images of E0102-72 and noted the radial variation with energy bands centered on OVII and OVIII, suggesting an ionizing shock propagating inward. The analysis of the high resolution dispersed spectrum, discussed below, reinforces this interpretation. In addition, Doppler shifts in the high-resolution spectrum give us a first look at the velocity structure.

2. The Observations

The supernova remnant E0102-72 was observed with the *Chandra* High Energy Transmission Gratings (HETG) in two segments as part of the guaranteed time observation program. The configuration included HETG with the Advanced CCD Imaging Spectrometer (ACIS-S). ACIS has moderate spectral resolution which allows order sorting of the grating spectrum. The two E0102-72 observations had slightly different roll angles and aim points. Most of the analysis below was therefore restricted to a single observation (Obsid 120).

Table 1. HETG observations of E0102-72.

| | |
|---------------|-------------|
| Obsid 120 | Obsid 968 |
| 90 ksec | 48.6 ksec |
| Sept 28, 1999 | Oct 8, 1999 |

3. The High Resolution X-Ray Spectrum

A portion of the dispersed high resolution X-ray spectrum of E0102-72 (a thousand year old supernova remnant in the Small Magellanic Cloud) is shown in Figure 1. The *Chandra* observation was taken using the High Energy Transmission Grating Spectrometer (HETGS) which employs the High Energy Gratings in conjunction with the Advanced CCD Imaging Spectrometer (ACIS). The HETGS separates the X-rays into their distinct X-ray emission lines, forming separate images of the remnant with the X-ray light of each line. The dispersed spectrum shows X-ray lines of highly ionized oxygen, neon, magnesium and silicon. Several of the dispersed ‘ring’ images differ from the zeroth order image. There are differences in radii, likely caused by the changing ionization state, that suggest the passage of the supernova ejecta through the reverse shock. Note also the distorted shape of the NeX Ly α line relative to the zeroth order. This is due to Doppler shifts associated with high velocity material. Both of these features are discussed in detail below.

4. The Ionization/Shock Structure of E0102-72: Measurements

A side-by-side comparison of the dispersed OVII resonance line with the OVIII Ly α line is given in Figure 2. OVII is helium-like oxygen, with two electrons remaining, whereas OVIII is hydrogen-like. The ring diameter of the OVIII line is obviously larger than that of the OVII line.

The ring diameters for all the bright X-ray lines were measured by tracing the distribution in the cross-dispersion direction, as illustrated in the right panel of Figure 2, which shows the cross-dispersion histograms for the OVIII Ly α and OVII resonance lines. Each histogram begins below the bottom edge of the ring and ends above the top edge. Clearly, the diameters of the two rings differ markedly, with the helium-like OVII being narrower.

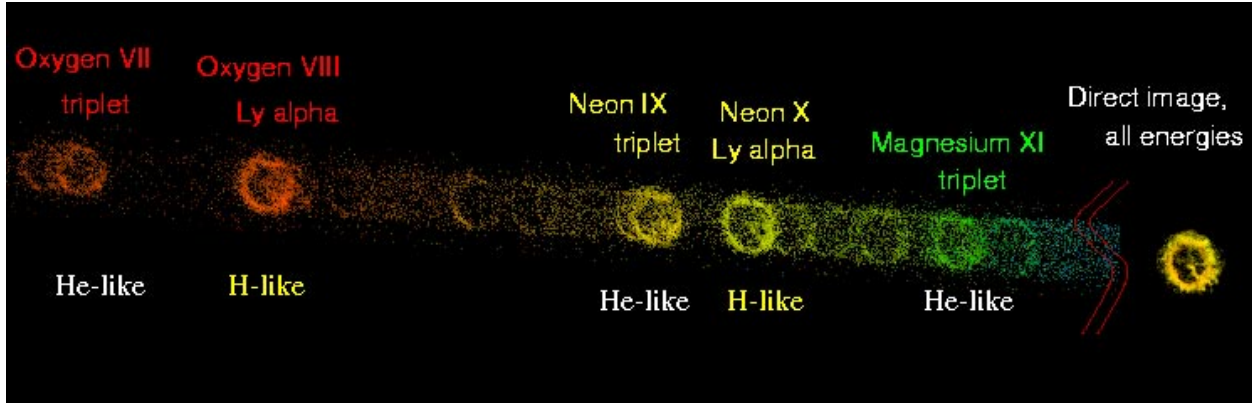


Figure 1. Dispersed high resolution X-ray spectrum of E0102-72. Shown here is a portion of the -1 order formed by the medium energy gratings, color coded to suggest the ACIS energy resolution. At right in the figure is the zeroth order, which combines all energies in an undispersed image. Differences in radii (as seen contrasting OVIII with OVII) and distortions in the shape (as seen in NeX Ly α) are significant, reflecting progress of the reverse shock and Doppler shifts, respectively. The resonance line of helium-like silicon is not shown in the figure.

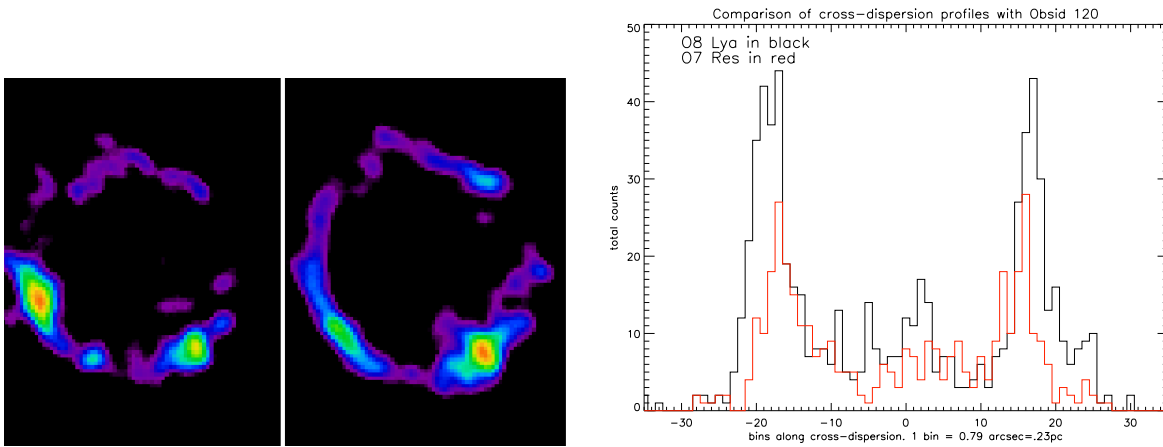


Figure 2. The dispersed image formed by the OVII resonance line (574 eV) is shown at far left next to that of the OVIII Ly α line (654 eV), which is shown to its immediate right on the same scale. The radius of the helium-like OVII line is obviously smaller than that of the hydrogen-like OVIII line. The right-hand panel overlays the cross-dispersion histograms of these two images. The histogram of the OVII line (in red) is nestled inside that of the OVIII line (in black). These histograms provided numerical measures of ring diameters as plotted in Figure 3.

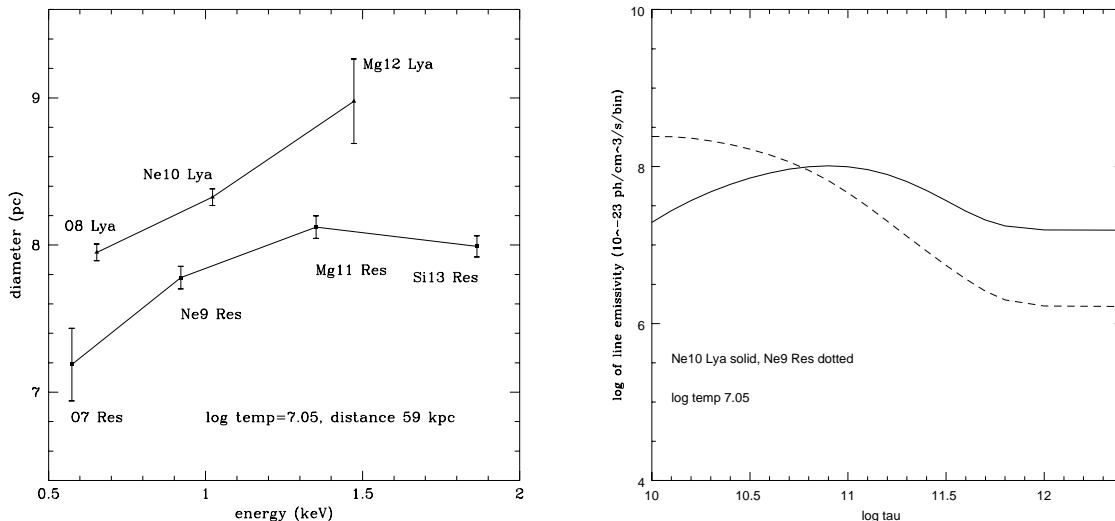


Figure 3. **Left:** The ring diameters for the bright lines are plotted against energy. The top curve connects the hydrogen-like lines, and the bottom curve connects the helium-like lines. Note that the hydrogen-like lines lie outward of their helium-like counterparts, regardless of element. **Right:** The emissivity of a helium-like line peaks earlier than that of a hydrogen-like line in an ionizing plasma.

The measured diameters for the bright lines are shown in the Figure 3. It is apparent that **all of the hydrogen-like lines** (connected by the top curve) **lie outside their corresponding helium-like lines** (connected by the bottom curve). As each element is considered on an individual basis, the hydrogen-like emitting region lies outward of the helium-like emitting region, suggesting a mechanism which is independent of spatial separation of the elements. This mechanism is discussed in the next section.

5. The Ionization/Shock Structure of E0102-72: Model

Consider the evolution of an ionizing plasma toward equilibrium. After the passage of a shock, at a fixed electron temperature T_e and electron density n_e , a helium-like ionization state is created earlier than a hydrogen-like state. This is illustrated in the right panel of Figure 3, where a neon plasma has been heated to electron temperature $T_e=10^{7.05}$ by the passage of a shock. The emissivity of a line of helium-like neon is seen to peak at an earlier ionization age than hydrogen-like neon (where the ionization age τ is defined as the product of electron density n_e and time since passage of the shock, i.e., $\tau=n_e t$). The hydrogen-like outer region is therefore a more ‘evolved’ plasma than the helium-like inner region. This suggests the action of a shock moving *inward* relative to the ejecta - the ‘reverse shock’ - which is the standard model for the mechanism which heats SNR ejecta to X-ray temperatures. This is illustrated in the left panel of Figure 4.

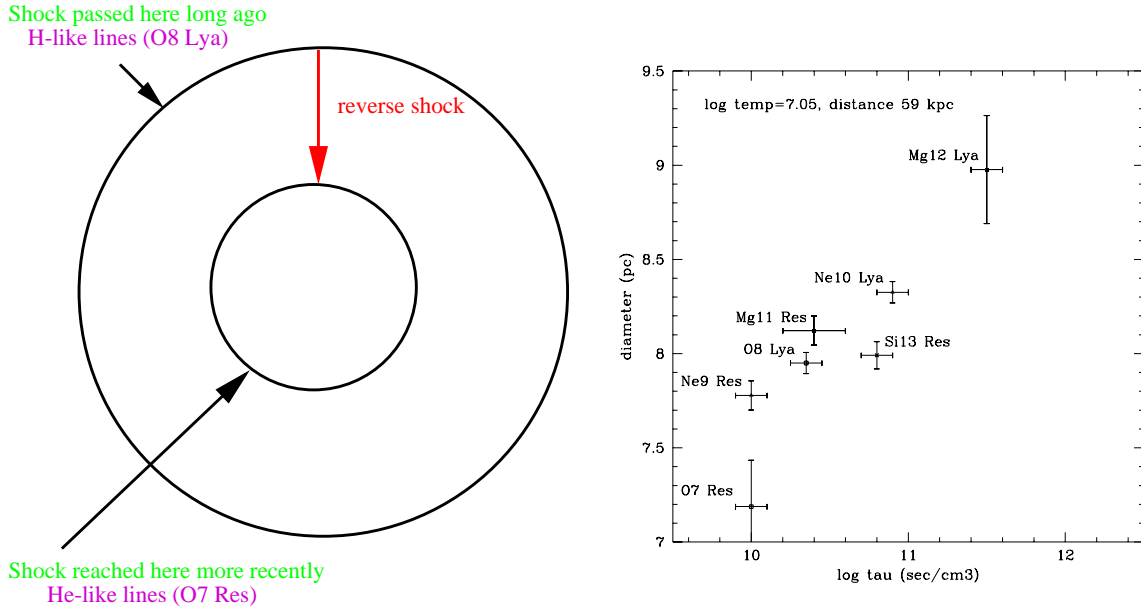


Figure 4. The panel at left illustrates how the progress of the ‘reverse shock’ results in the more-evolved (hydrogen-like) plasma lying outward of the less-evolved (helium-like) plasma. The panel at right shows the results of applying of a simple model. Ring diameter and ionization age are seen to be correlated, lending credence to the interpretation that diameter differences are the result of ionization structure resulting from the ‘reverse shock’. (The plotted point for OVII Res is an upper limit.)

The results of applying a very simple model are shown in the right panel of Figure 4. The model assumes that the elements are uniformly mixed, and that there is a single electron temperature. We make these assumptions to examine the proposition that the ring diameter corresponds to ionization age, where we have estimated that age by finding the peak emissivity (Raymond & Smith 1977; Hughes & Helfand 1985) for each bright X-ray line assuming a fixed T_e of about 1 keV or $\log T_e = 7.05$ (as suggested by our global NEI analysis). Although any workable model must consider many parameters, the monotonic behavior of the data strongly suggests that these arcsec differences in ring diameter are attributable to the ionization structure resulting from the reverse shock.

6. The Velocity Structure of E0102-72

As seen in Figure 5, distortion is evident when dispersed images of NeX Ly α are compared with the zeroth order ($m=0$). (The zeroth order has been filtered to include only events around the 1022 eV energy of NeX Ly α). The leftmost panel shows the $m=-1$ ring, the middle panel is the zeroth order, and the right panel is the $m=+1$ ring. Doppler red shifts to longer wavelengths are indicated by distortions outward, away from zero order, and blue shifts are indicated by distortions of the ring *toward* the zeroth order at the center. Thus,

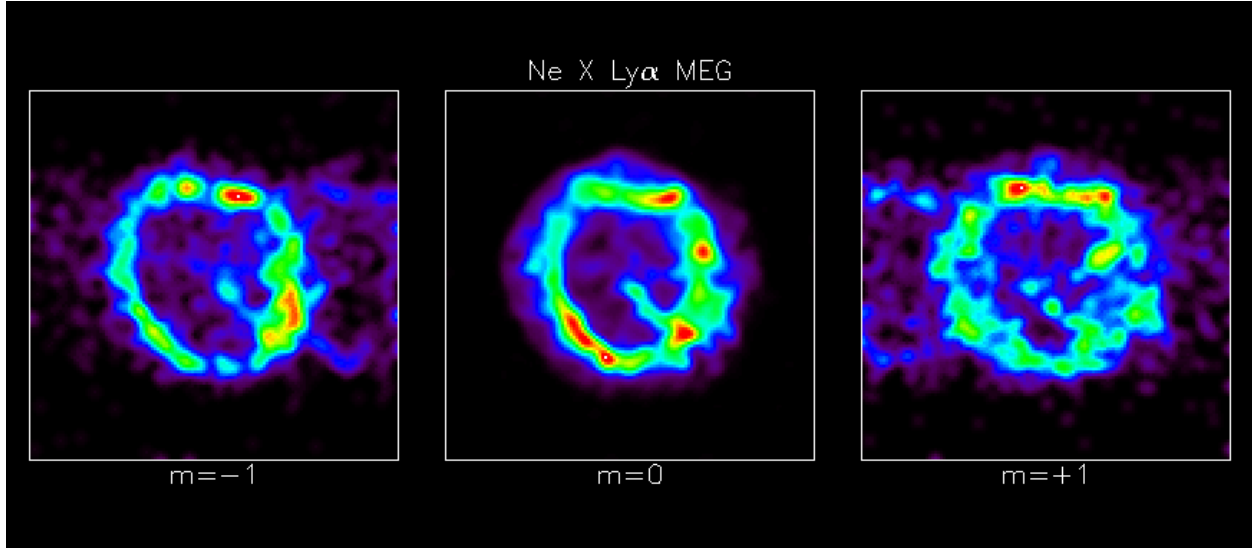


Figure 5. The dispersed $m=-1$ and $m=+1$ orders of NeX Ly α show distortions relative to the undispersed zero ($m=0$) order. These distortions are attributed to Doppler shifts.

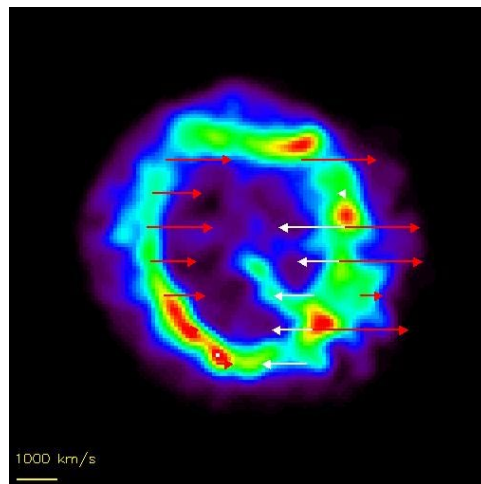


Figure 6. Schematic Doppler map of E0102-72 as detected with NeX Ly α . The lengths and locations of the arrows are used to indicate the relative velocities and approximate locations associated with the Doppler shifts. White arrows pointing left represent blue shifts; red arrows pointing right represent red shifts.

the upper left sector of the remnant appears to have a red shift as seen by examining the $m=-1$ order ring, whereas the right half of the ring is broadened in the $+1$ order, indicating *both* red and blue shifts for the right half of the remnant. KS tests support this qualitative interpretation, indicating that, to high confidence, the dispersion-direction profiles of the dispersed and undispersed images are *different*, while the cross-dispersion profiles are *the same*.

The results of quantitative analysis are schematically illustrated in Figure 6, where white arrows pointing toward the left indicate blue shifts, and red arrows pointing toward the right indicate red shifts. The lengths and locations of the arrows are used to indicate the relative velocities and approximate locations associated with the Doppler shifts. Typical red and blue-shifts indicate velocities on the order of 1000 km/s (Houck et al. 2000), comparable to those of optical filaments.

7. Conclusions

The *Chandra* high-resolution X-ray spectrum of E0102-72 obtained with the HETGS reveals images of the supernova remnant in the light of individual lines of O, Ne, Mg and Si. Radial variations among different ionization stages are seen on an arcsecond spatial scale, consistent with an evolving ionization structure due to the passage of the ejecta through the reverse shock. Doppler shifts of ~ 1000 km/sec (comparable to the velocities of optical filaments) have been detected at various locations along the remnant. This velocity information is being applied toward a model of the morphology and motion of the X-ray emitting material.

Acknowledgments. We thank Glenn Allen, Norbert Schulz, Tom Pannuti and Sara-Anne Taylor for helpful discussions. We are grateful to the CXC group at MIT for their assistance in analysis of the data. This work was prepared under NASA contract NAS8-38249 and SAO SV1-61010.

References

- Amy, S.W. & Ball, L. 1993, ApJ, 411, 761
 Blair, W.P., Raymond, J.C., Danziger, J. & Matteucci, F. 1989, ApJ, 338, 812
 Blair, W.P., Morse, J.A., Raymond, J.C., Kirshner, R.P., Hughes, J.P., Dopita, M.A., Sutherland, R.S., Long, K.S. & Winkler, P.F. 2000, ApJ, 537, 667
 Dopita, M.A., Tuohy, I.R. & Mathewson, D.S. 1981, ApJ, 248, L105
 Flanagan, K.A., et al. 2000, in preparation
 Gaetz, T.J., Butt, Y.M., Edgar, R.J., Eriksen, K.A., Plucinsky, P.P., Schlegel, E.M. & Smith, R.K. 2000, ApJ, 534, L47
 Hayashi, I., Koyama, K., Masanobu, O., Miyata, E., Tsunemi, H., Hughes, J.P. & Petre, R. 1994, PASJ, 46, L121
 Houck, J.C., et al. 2000, in preparation
 Hughes, J.P. & Helfand, D.J. 1985, ApJ, 291, 544

- Hughes, J.P. 1988, in *Supernova Remnants and the Interstellar Medium*, ed. R.S. Roger & T.L. Landecker (Cambridge: Cambridge Univ. Press), 125
- Hughes, J.P., Rakowski, C.E. & Decourchelle, A. 2000, *ApJ*, in press
- Tuohy, I.R. & Dopita, M.A. 1983, *ApJ*, 268, L11
- Raymond, J.C. & Smith, B.W. 1977, *ApJS*, 35, 419
- Seward, F.D. & Mitchel, M. 1981, *ApJ*, 243, 736